



Universiteit
Leiden
The Netherlands

Far-infrared observations of the Crab nebula

Marsden, P.L.; Gillett, F.C.; Jennings, R.E.; Emerson, J.P.; Jong, T. de; Olnon, F.M.

Citation

Marsden, P. L., Gillett, F. C., Jennings, R. E., Emerson, J. P., Jong, T. de, & Olnon, F. M. (1984). Far-infrared observations of the Crab nebula. *Astrophysical Journal*, 278, L29-L32. Retrieved from <https://hdl.handle.net/1887/6454>

Version: Not Applicable (or Unknown)

License:

Downloaded from: <https://hdl.handle.net/1887/6454>

Note: To cite this publication please use the final published version (if applicable).

FAR-INFRARED OBSERVATIONS OF THE CRAB NEBULA¹

P. L. MARSDEN, F. C. GILLET, R. E. JENNINGS, J. P. EMERSON, T. DE JONG, AND F. M. OLNON

Received 1983 September 12; accepted 1983 November 21

ABSTRACT

Infrared photometry for the total flux from the Crab nebula using the *Infrared Astronomical Satellite (IRAS)* survey detectors is presented. The observations show an infrared excess beyond $12\ \mu\text{m}$ over the extrapolated radio and near-infrared fluxes. The break in the radio spectrum occurs at approximately $1 \times 10^{13}\ \text{Hz}$, consistent with an average magnetic field strength of roughly 300 microgauss. The luminosity excess is approximately $1000\ L_{\odot}$ and is interpreted as due to thermal emission from $5\text{--}30 \times 10^{-3}\ M_{\odot}$ of dust in the nebula.

Subject headings: infrared: sources — nebulae: Crab Nebula

I. INTRODUCTION

Although the emission spectrum of the Crab nebula has been the subject of numerous investigations covering 13 decades in frequency, the detailed linking up between the visible and radio regions of the spectrum is still unclear. The radio spectrum from 10^8 to $3 \times 10^{10}\ \text{Hz}$ has an accurately defined slope, $f_{\nu} \propto \nu^{-\alpha}$ with $\alpha = 0.263$ (Baars and Hartsuijker 1972), while at higher frequencies the observations at $2.2 \times 10^{10}\ \text{Hz}$ (Janssen, Golden, and Welch 1974), at $3 \times 10^{11}\ \text{Hz}$ (Werner *et al.* 1977), and at $10^{12}\ \text{Hz}$ (Wright *et al.* 1979) are consistent with an extension of this simple power law. Observations spanning the visible and the ultraviolet after large corrections for interstellar extinction exhibit a spectrum with a slope $\alpha \sim 0.5$ (Scargle 1969; Kirshner 1974; Wu 1981; Davidson *et al.* 1982). Observations in the near-infrared ($\sim 1\ \mu\text{m}$) have generally been considered to be consistent with the visible-ultraviolet data.

The frequency at which the radio spectrum turns over toward the visible is a basic parameter in synchrotron models of the radio emission from the nebula and under certain simplifying assumptions leads to a value for the average magnetic field strength in the nebula. A wide range of values for the break frequency has been deduced in the past by extrapolating from the shorter wavelength observations. The *IRAS* observations reported here add new information in the range of frequencies where the break is expected to occur.

Another aspect of Crab nebula investigations is related to the modeling of supernova explosion and the subsequent expansion of the remnants into the interstellar medium. Dwek and Werner (1981) have, for example, recently investigated the heating of the grains following supernova explosions and, in the case of the Crab nebula, have estimated the mass of dust contained within the nebula to be approximately $0.01\text{--}0.04\ M_{\odot}$, using as input data the upper limits to the flux densities at 100 and $50\ \mu\text{m}$ reported by Harvey, Gatley, and Thronson

(1978). With the *IRAS* observations, we are able to establish firm values for these flux densities and thereby improve upon the estimates of the dust temperature and the mass of dust contained within the nebula.

II. OBSERVATIONS AND RESULTS

The observations were made during the period 1983 March 9–16. Data taken from three survey scans across the nebula have been used in the analysis. The nebula is an extended object, so that as its image is swept across the focal plane, up to three detectors in cross scan in each wave band may be illuminated at any one time. To obtain the integrated flux for the whole nebula, we have summed the signals from appropriate and adjacent cross-scan detectors (allowing for overlap and the baseline level). The summed signals are converted to flux densities as described by Neugebauer *et al.* (1984). The results from the three scans are given in Table 1.

The scans crossed the focal plane in different positions, illuminating different sets of detectors for each scan. Thus, depending upon exactly how the scan track crossed the focal plane (in some cases crossing detectors which were off), one or two independent measurements of the infrared radiation were available in each band for each scan. The uncertainties in the averages given in Table 1 are the random $1\ \sigma$ values and do not include systematic uncertainties.

The results of detailed mapping of the infrared emission are not yet available although the survey observations reported here indicate that the infrared emitting region has a comparable extent to the optical size of the nebula.

III. DISCUSSION

In Figure 1, we plot the flux densities ($\log f_{\nu}$) from Table 1, against \log (frequency), together with observations for the radio, near-infrared, visible, and ultraviolet regions of the spectrum. We have arbitrarily assigned $\pm 20\%$ error bars to the *IRAS* values which generously allows for the absolute uncertainties in the *IRAS* calibrations (Neugebauer *et al.* 1984). For the near-infrared through to the ultraviolet, correc-

¹The *Infrared Astronomical Satellite* used in these observations was developed and is operated by the Netherlands Agency for Aerospace Programs (NIVR), the US National Aeronautics and Space Administration (NASA), and the UK Science and Engineering Research Council (SERC).

TABLE 1
THE 12–100 MICRON FLUX DENSITY FOR THE CRAB NEBULA

	λ (μm)			
ν (Hz)	12	25	60	100
LOG (ν)	2.5×10^{13}	1.2×10^{13}	5×10^{12}	3×10^{12}
SCAN NO.	13.40	13.08	12.70	12.48
1: f_ν (Jy)	41.4	95.6	210	235
	206
2: f_ν (Jy)	44.2	99.2	210	206
	...	97.1	215	210
3: f_ν (Jy)	46.7	100.5	206	231
	209
Average f_ν (Jy) ...	44.1	98.1	210	216
Average σ (Jy) ...	2.6	2.2	3.4	13

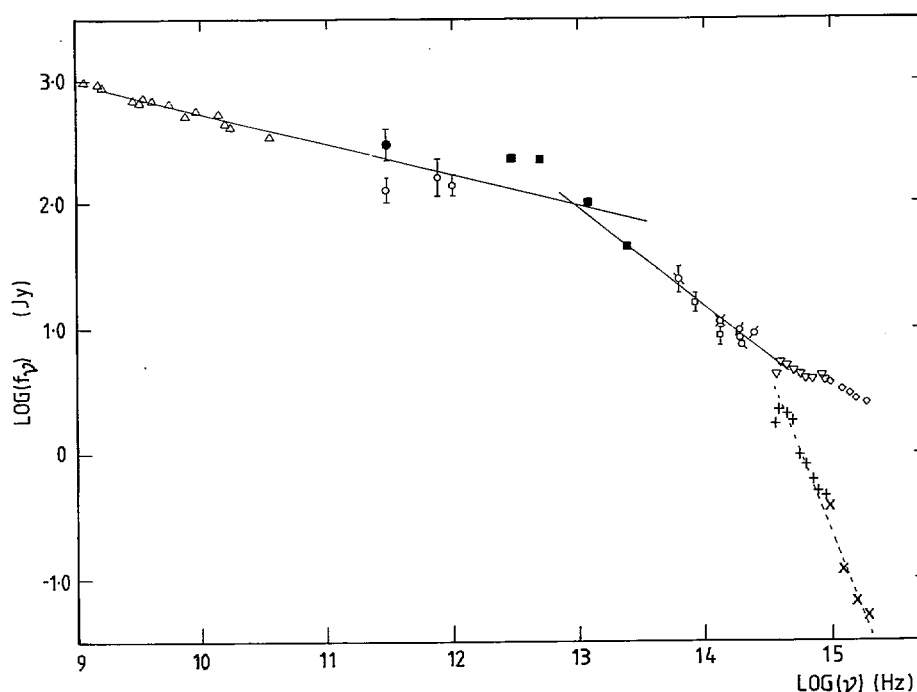


FIG. 1.—Radio, infrared, optical, and ultraviolet spectrum of the Crab nebula. Data are from the following sources: Δ , Baars and Hartsuiker (1972); \bullet , Werner *et al.* (1977); \circ , Wright *et al.* (1979); \blacksquare , *IRAS*; open circle with \backslash diagonal, Grasdalen (1979); \square , Ney and Stein (1968); open circle with / diagonal, Becklin and Kleinmann (1968); ∇ , Scargle (1969), corrected for extinction; $+$, Scargle (1969), uncorrected for extinction; \diamond , Wu (1981), corrected for extinction; \times , Wu (1981), uncorrected for extinction.

tions are necessary for the interstellar extinction, and we have used the data as corrected by Wu (1981). No extinction corrections have been made to the *IRAS* data. (These are less than the assumed uncertainties.) The uncorrected data in the visible and ultraviolet are also plotted to show the scale of the extinction corrections which have been applied. These vary from a factor of approximately $\times 2$ in the visible to a factor of approximately $\times 50$ in the far-ultraviolet.

The *IRAS* 12 μm observations at 2.5×10^{13} Hz, together with observations in the near-infrared and the long-wavelength end of the visible, lie on a straight line of slope $\alpha \sim 0.8$. It is not clear whether this is significantly different from the slope $\alpha = 0.5$ in the visible and ultraviolet which Wu (1981) reported, since the degree of uncertainty arising from the

extinction corrections in this part of the spectrum tends to emphasize the change of slope. Kirshner (1974) has shown, for example, that varying the visual extinction A_v from 1.8 to 1.4 causes the slope of the corrected visual observations to vary between $\alpha = 0.17$ and $\alpha = 0.5$.

The extrapolated line through the *IRAS* observations intercepts the projected radio-frequency spectrum at the break frequency, $\nu_b \sim 1 \times 10^{13}$ Hz. The break frequency is related to the average magnetic field strength and the lifetime against synchrotron energy losses of the electrons emitting the radiation according to the relation

$$\nu_b (\text{GHz}) = 3.5 \times 10^{17} / B^3 (\mu\text{G}) t^2 (\text{yr}), \quad (1)$$

and with t equal to the time interval since the Crab outburst

(930 years), with $\nu_b = 1 \times 10^{13}$ reported here, we find that B is approximately $300 \mu\text{G}$. This is consistent with earlier evaluations (in the range 5×10^3 to $10^2 \mu\text{G}$), but it is probably defined more accurately than previously. With $B = 300 \mu\text{G}$ and the conventional synchrotron model (i.e., a power-law differential electron energy spectrum), where the electron power-law index $\gamma = 2\alpha + 1 = 1.5$ (from the radio spectrum), and equality between the magnetic and particle energy densities, the steepening in the electron spectrum occurs at approximately 80 GeV .

We next consider the infrared luminosity from the nebula. In Figure 1, the $60 \mu\text{m}$ and $100 \mu\text{m}$ *IRAS* fluxes show an excess over the extrapolated radio spectrum. The 50 – $100 \mu\text{m}$ flux is at least twice as large as the extrapolated radio flux and is well outside the calibration uncertainties at these wavelengths. The $25 \mu\text{m}$ band shows an excess over the spectrum extrapolated up from the visible through the near-infrared.

Figure 2 shows this excess for the four *IRAS* wave bands. The excess at $12 \mu\text{m}$ is essentially zero, and we have taken as an upper limit to the excess in this band the 1σ uncertainty limit of 2.6 Jy ($\sim 5\%$ of the observed signal). The uncertainties in the other bands correspond to the 20% values referred to earlier. The infrared luminosity derived from the integrated excess is approximately $10^3 L_\odot$, where we have taken the distance to the nebula to be 2 kpc . The total luminosity of the Crab nebula is approximately $2.5 \times 10^4 L_\odot$, of which 60% is emitted in the ultraviolet, X-ray, and gamma-ray regions (Wilson and Weiler 1976; Parlier *et al.* 1974), and heating of the dust grains (which requires only $\sim 4\%$ of the total luminosity) is probably due to this shorter wavelength radiation.

Also shown in Figure 2 are two blackbody curves calculated for $T = 70$ and 100 K with an emissivity $\epsilon \propto \nu$. Comparison of the *IRAS* points with these curves suggests that the infrared excess is due to heated dust with temperatures ranging between 70 and 100 K , but close to 70 K . For the discussion, we use 80 K as a representative value. If the emissivity is taken to vary as ν^2 , then the excess can be fitted with T in the 40 – 60 K range, although the fit is not as good as for $\epsilon \propto \nu$.

Dwek and Werner (1981) have modeled the infrared emission from supernova condensates and examined the heating effects due to the X-radiation field in the Crab nebula. They consider two types of grain, (1) with $\epsilon \propto \nu$ and (2) with $\epsilon \propto \nu^2$, and deduce the equilibrium temperatures for the two types of grains. For type (1), $T = 26a^{-0.2}$, where a is the grain radius in microns, and for type (2) $T = 51a^{-0.33}$. With $T = 80 \text{ K}$ for type (1), we find $a \sim 0.004 \mu\text{m}$, and for type (2) with $T = 50 \text{ K}$, $a \sim 1 \mu\text{m}$. Following Dwek and Werner, these give for the total mass of dust in the nebulae, M_d , for type (1) grains $M_d \sim 5 \times 10^{-3} M_\odot$, and for type (2), $M_d \sim 0.8 M_\odot$. In these estimates, it is assumed that the grains achieve a constant equilibrium temperature, but for the very small and cold grains (i.e., grains with small thermal capacities), the grain temperature will fluctuate considerably following the absorption of each UV–X-ray photon (Aannestad and Kenyon 1979). It is beyond the intent of this Letter to investigate this in detail, but the general effect would be to increase the estimate for the mass of dust in the nebula.

The values of M_d deduced above may be compared with estimates based upon the evaluation of the optical depth at

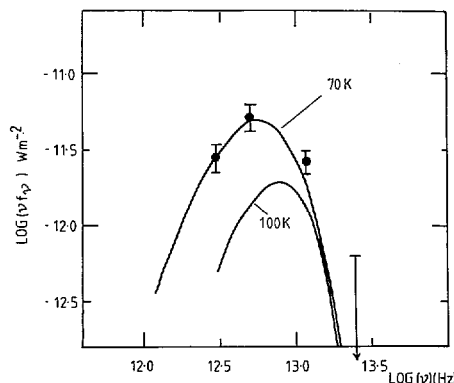


FIG. 2.—Infrared excess in the Crab nebula. *IRAS* data points are shown. Curves represent νB_ν (70 K) and νB_ν (100 K) spectra.

$100 \mu\text{m}$, using the excess flux at $3 \times 10^{12} \text{ Hz}$ reported here ($94 \pm 20 \text{ Jy}$) and an assumed mass absorption coefficient of $250 \text{ cm}^2 \text{ g}^{-1}$ (Campbell, Hoffmann, and Thronson 1981, based upon the work of Day 1976). We find that, for type (1) grains with $T = 80 \text{ K}$, $\tau_{100} = 5 \times 10^{-6}$, $M_d \sim 10^{-3} M_\odot$; and for type (2) grains with $T = 50 \text{ K}$, $\tau_{100} = 5 \times 10^{-3}$, and $M_d \sim 0.3 M_\odot$, where we have assumed the dimensions of the nebula to be $7' \times 5'$.

The high values of M_d for type 2 dust appear excessive in relation to the estimated $2.5 M_\odot$ of helium and hydrogen in the nebula (Davidson *et al.* 1982), although they do not contravene the limits 0.5 – $1.0 M_\odot$ set by the extinction observations of Trimble (1977). In addition, the existence of large $1 \mu\text{m}$ grains which the larger mass of dust implies appears most unlikely among supernova remnants. It is also not clear that it is valid to use an emissivity variation proportional to ν^2 at the *IRAS* wavelengths. The variation of $\epsilon \propto \nu^2$ is usually invoked for wavelengths greater than approximately $250 \mu\text{m}$. We therefore consider that estimates based on $\epsilon \propto \nu$ giving a lower value for M_d are likely to be more representative of the actual nebula. In this case, the infrared-excess data points in Figure 2 cannot be fitted with a temperature less than 40 K . With $T = 40 \text{ K}$ and $\epsilon \propto \nu$, the mass of dust is calculated to be $0.03 M_\odot$, using the Dwek and Werner (1981) analysis. Higher temperatures, of course, lead to smaller values for M_d , and we therefore adopt $M_d \sim 0.03 M_\odot$ as a reasonable upper limit to the mass of dust.

It is of interest to see if it is possible, using the new data, to determine whether the dust in the nebula originated in the supernova or came from the interstellar medium (ISM). The mass of dust swept up from the ISM may be estimated using the extinction observations made in the vicinity of the Crab (Trimble 1977) and an expansion time of 1000 years. The mass of dust calculated in this way is approximately $0.002 M_\odot$, which is 15 times smaller than the upper limit for M_d ($0.03 M_\odot$) reported here but is within a factor of 2 of the lower limit ($0.005 M_\odot$). Thus, although the present observations generally favor the supernova or stellar precursor shell as the source of the dust, we cannot unambiguously rule out the ISM as the source.

Using $M_d \sim 0.03 M_\odot$, the gas to dust mass ratio within the nebula is approximately 100 (with $M_{\text{gas}} = 2.5 M_\odot$), and the upper limit to this ratio is approximately 500 with $M_d = 5 \times$

$10^{-3} M_{\odot}$. These values span the range usually accepted for the ISM and less dense clouds and run counter to the suggestion of Dwek and Werner (1981) that supernova ejecta are a most important source of stellar grains.

We are pleased to acknowledge the help of the Preliminary Analysis Facility data processing team, without whose help this work would not have been possible.

REFERENCES

- Aannestad, P. A., and Kenyon, S. J. 1979, *Ap. J.*, **230**, 771.
 Baars, J. W. M., and Hartsuijker, A. P. 1972, *Astr. Ap.*, **17**, 172.
 Becklin, E. E., and Kleinmann, D. E. 1968, *Ap. J. (Letters)*, **152**, L25.
 Campbell, M. F., Hoffmann, W. F., and Thronson, H. A. 1981, *Ap. J.*, **247**, 530.
 Davidson, K., et al. 1982, *Ap. J.*, **253**, 696.
 Day, K. L. 1976, *Ap. J.*, **210**, 614.
 Dwek, E., and Werner, M. W. 1981, *Ap. J.*, **248**, 138.
 Grasdalén, G. L. 1979, *Pub. A.S.P.*, **91**, 436.
 Harvey, P. M., Gatley, I., and Thronson, H. A. 1978, *Pub. A.S.P.*, **90**, 655.
 Janssen, M. A., Golden, L. M., and Welch, W. J. 1974, *Astr. Ap.*, **33**, 373.
 Kirshner, R. P. 1974, *Ap. J.*, **194**, 323.
 Neugebauer, G., et al. 1984, *Ap. J. (Letters)*, **278**, L1.
 Ney, E. P., and Stein, W. A. 1968, *Ap. J. (Letters)*, **152**, L21.
 Parlier, B., et al. 1974, *Supernova and Supernova Remnants* ed. C. B. Cosmovici (Dordrecht: Reidel), p. 267.
 Scargle, J. D. 1969, *Ap. J.*, **156**, 401.
 Trimble, V. 1977, *Ap. Letters*, **18**, 145.
 Werner, M. W., Neugebauer, G., Houck, J. R., and Hauser, M. G. 1977, *Pub. A.S.P.*, **89**, 127.
 Wilson, A. S., and Weiler, K. W. 1976, *Astr. Ap.*, **49**, 357.
 Wright, E. L., Harper, D. A., Hildebrand, R. H., Keene, J., and Whitcomb, S. E. 1979, *Nature*, **279**, 703.
 Wu, C.-C. 1981, *Ap. J.*, **245**, 581.